Model To Determine a Distinct Rate Constant for Carrier Multiplication from Experiments

Spoor, Frank; Grimaldi, Gianluca; Kinge, Sachin; Houtepen, Arjan; Siebbeles, Laurens

DOI
10.1021/acsaem.8b01779

Publication date
2019

Document Version
Final published version

Published in
ACS Applied Energy Materials

ACS APPLIED ENERGY MATERIALS

Article

Cite This: ACS Appl. Energy Mater. 2019, 2, 721−728

www.acsaem.org

Model To Determine a Distinct Rate Constant for Carrier Multiplication from Experiments

Frank C. M. Spoor,[†,§] Gianluca Grimaldi,[†,§] Sachin Kinge,[‡] Arjan J. Houtepen,*[,†] and Laurens D. A. Siebbeles*[,†]

[†]Optoelectronic Materials Section, Department of Chemical Engineering, Delft University of Technology, Van der Maasweg 9, 2629 HZ Delft, The Netherlands

[‡]Toyota Motor Europe, Materials Research & Development, Hoge Wei 33, B-1930, Zaventem, Belgium

Supporting Information

ABSTRACT: Carrier multiplication (CM) is the process in which multiple electron−hole pairs are created upon absorption of a single photon in a semiconductor. CM by an initially hot charge carrier occurs in competition with cooling by phonon emission, with the respective rates determining the CM efficiency. Up until now, CM rates have only been calculated theoretically. We show for the first time how to extract a distinct CM rate constant from experimental data of the relaxation time of hot charge carriers and the yield of CM. We illustrate this method for PbSe quantum dots. Additionally, we provide a simplified method using an estimated energy loss rate to estimate the CM rate constant just above the onset of CM, when detailed experimental data of the relaxation time is missing.

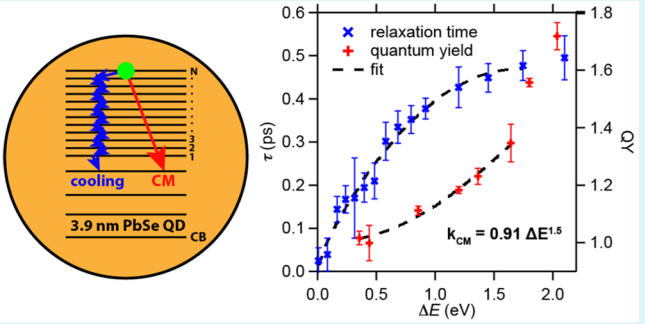

KEYWORDS: *carrier multiplication, electron−hole pairs, quantum dots, semiconductor, quantum yield*

INTRODUCTION

Absorption of a sufficiently energetic photon in a semiconductor can initially create a hot electron−hole pair with the electron and/or the hole having excess energy exceeding the band gap. Such hot charge carriers can cool down to the band edge by phonon emission, and in addition by excitation of one or more additional electrons across the band gap. The latter process of carrier multiplication (CM) leads to generation of two or more electron−hole pairs for one absorbed photon.[1,2]

In the past decade, many nanomaterials with varying composition, size and shape have been investigated for the occurrence of CM.[1−3] CM has been found in 0D quantum dots (QDs) in solution[4] and in thin films,[5,6] 1D nanorods,[7] 2D nanosheets,[8] 2D percolative networks[9] and bulk material.[10] CM is a promising process to increase the efficiency of solar energy conversion and has been demonstrated to occur in photovoltaic devices and solar fuel cells based on 0D, 1D or 2D nanomaterials.[11−15]

The quantum yield (QY) for charge carrier photogeneration (number of charges carriers per absorbed photon) is the net result of the competitive relaxation of a hot electron−hole pair via CM and cooling by phonon emission. Therefore, the competition between CM and cooling has been studied intensively.[16−19] Relaxation times have been experimentally determined in many materials, with a particular focus on lead selenide (PbSe) QDs, owing to their well-controlled synthesis and large range of possible band gap energies through tuning their size.[20] The outcome is that cooling at high energies relevant to CM is similar in QDs and bulk material.[21−23] However, according to theoretical calculations CM rates in QDs differ from those for bulk.[24−27]

While quantitative models describing experimental CM QY data via a competition between CM and cooling exist,[18,19] they employ strong assumptions on the energy dependence of CM and cooling rates. To our knowledge the most comprehensive study aimed at finding CM and cooling rates by theoretical analysis of measured QYs is that of Stewart et al.[18] However, in that work the rates were taken to be independent of the energy of the charge carrier. This assumption does not agree with the aforementioned theoretical calculations, which indicate that the CM rate strongly depends on charge carrier energy. In addition, our earlier work shows that the cooling rate also depends on energy. A model that allows one to extract an energy-dependent CM rate from experiments would be very valuable for the understanding of the factors that govern CM.

In this work, we derive a method to extract an energy-dependent CM rate constant from experimental measurements of the relaxation time of hot charge carriers to band edge states and the QY of electron−hole pairs. The method is valid up to a carrier excess energy (the energy of the carrier above the band

Received: October 18, 2018
Accepted: December 13, 2018
Published: December 13, 2018

DOI: 10.1021/acsaem.8b01779
ACS Appl. Energy Mater. 2019, 2, 721−728

edge, i.e., $E_{excess,e} = E_e - E_{CB}$ for electrons) of twice the band gap. In that case the hot charge carriers can undergo only one CM event. We use the method to determine an energy-dependent CM rate constant from our previous experimental data for PbSe QDs.[23] The method is however much more generally applicable and can be used to derive CM rate constants for any material of which experimental results of both the relaxation time and the QY are available. We also discuss a simplification to the method using an estimated energy loss rate instead of experimental data of the relaxation time. This simplified method can be used to find an estimate of the CM rate constant just above the energetic threshold of CM using only QY data when experimental data of the relaxation time of hot charge carriers is not available, as is the case for many materials that are studied for CM.

METHODS

Experimental Relaxation Time and QY. The carrier cooling data used in this work are taken from Spoor et al.,[23] where we reported energetic relaxation of electrons and holes to the band edges as a function of photoexcitation energy $h\nu$ for 3.9 nm PbSe QDs with a band gap of 0.95 eV. In that work, we determined accurately the relaxation time of the electrons, shown in Figure 1a as a function of photon energy. At photoexcitation energies relevant for CM, starting at twice the band gap energy, the relaxation time for electrons was found to increase continuously as a function of photoexcitation energy. The QY data are taken from Spoor et al., measured on the same 3.9 nm PbSe QDs used in the cooling study.[28] Figure 1b shows this QY as a function of photoexcitation energy normalized by the band gap energy. A straight line is fitted to the data points above unity to find the CM threshold at 2.7 times the band gap energy and a CM efficiency given by $\eta = \frac{QY - 1}{h\nu / E_{bg}} \times 100\% = 40\%$.

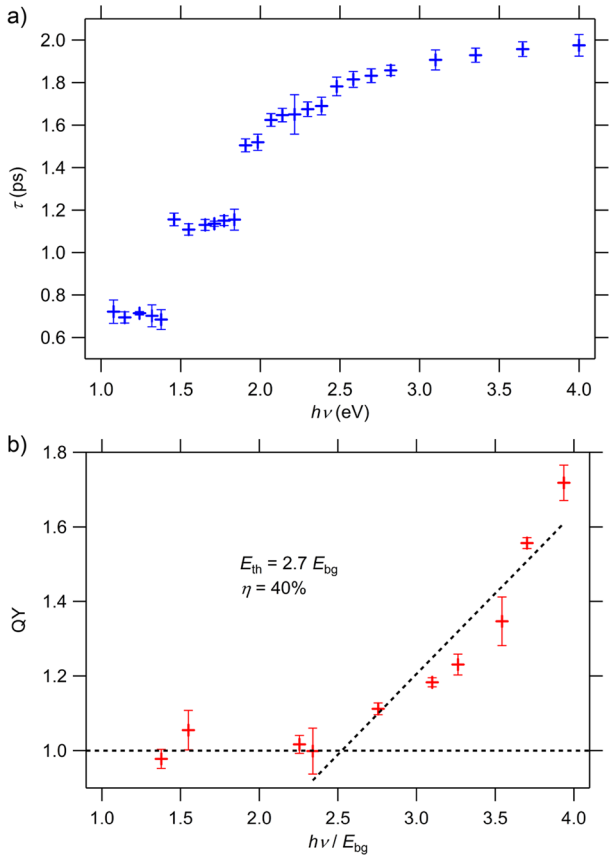

Figure 1. (a) Electron relaxation times as a function of photoexcitation energy and (b) QY as a function of photoexcitation energy scaled by the band gap energy for 3.9 nm PbSe QDs as reported in our previous works.[23,28]

Model of the Electronic Structure. From the data in Figure 1, we wish to extract a rate constant for CM. To do so we first need to define an electronic structure for PbSe QDs. Many calculations of the PbSe QD electronic structure exist,[23,29,30] yielding a high density of states (DOS) at energies relevant for CM. The situation of a high DOS ensures that electronic states are always available for energy conservation upon phonon emission by a charge carrier. Indeed, carrier relaxation was shown to be governed by phonon emission for charge carriers with high excess energy over the band gap, as occurs in bulk materials.[21−23] As an approximation, we can therefore use an electronic structure consisting of N equidistant energy levels, with the distance determined by the phonon energy, δE, at energies relevant for CM. We ignore the exact electronic structure near the band edge, since CM cannot occur from these energy levels. We show such an electronic structure in Figure 2a. We label the valence band (VB), conduction band (CB) and the higher energy levels (with indices 1 to N) from which CM can occur. Setting the CB energy to 0, the electron energy for which CM can occur must be at least one band gap energy E_{bg}. Taking into account only states relevant for CM, we take level 1 at an energy equal to E_{bg}. The highest energy level, at which we create a hot electron, is labeled N.

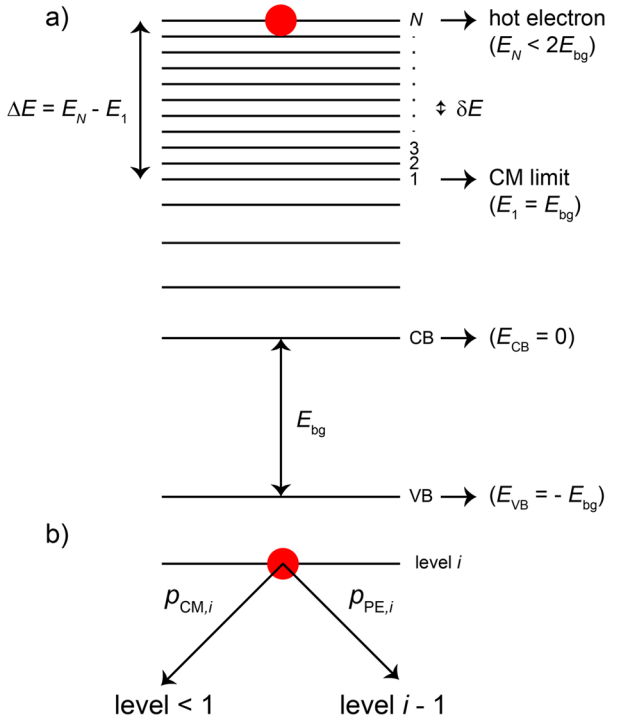

Figure 2. (a) Electronic structure for PbSe QDs. The CB energy is set to 0, such that the first energy level from which an electron can undergo CM has at least the band gap energy E_{bg}. This energy level is labeled 1. Above the minimal energy required for CM, we assume equidistant energy levels with N the highest level at which we initially create a hot electron. Since we only consider single CM events, this energy must be lower than twice the band gap energy. (b) Possible scenarios of phonon emission or CM from an energy level i.

In the electronic structure of Figure 2a, an electron in an energy level i has two possibilities. It either cools down to the energy level $i - 1$ below by emitting a phonon or undergoes CM, as illustrated in Figure 2b. Upon CM, it decays to a level $i < 1$. If the electron energy is larger than twice the band gap energy, the electron theoretically could undergo CM to a level $i \geq 1$ and hence undergo CM twice. We consider only single CM events and therefore consider the highest

DOI: 10.1021/acsaem.8b01779
ACS Appl. Energy Mater. 2019, 2, 721−728

carrier energy to be just below twice the band gap energy. This determines our limit for energy level N ($E_N < 2E_{bg}$). When an electron in our analysis decays to a level $i < 1$, it is not considered further, since CM is no longer energetically allowed. We now define $k_{PE,i}$ as the phonon emission rate constant from level i, $k_{CM,i}$ as the CM rate constant from level i, ΔE as the hot electron energy above the theoretical onset of CM (the electron energy in level N minus the electron energy in level 1) and δE as the phonon energy, which is the distance between energy levels, see Figure 2a. Since we assume that cooling is governed by phonon emission only, the overall relaxation rate constant equals $k_{tot,i} = k_{PE,i} + k_{CM,i}$. The probability to either emit a phonon, $p_{PE,i}$, or undergo CM, $p_{CM,i}$, from a certain level i is expressed in terms of the rate constants as

$$p_{PE,i} = \frac{k_{PE,i}}{k_{tot,i}}$$
$$p_{CM,i} = \frac{k_{CM,i}}{k_{tot,i}} \tag{1}$$

Calculation of the Relaxation Time and QY. Using the electronic structure of Figure 2a, we can now identify the possible relaxation scenarios of a hot electron from any energy level i between 1 and N. For example, if an electron is created in energy level 2, it can either (i) undergo CM directly, (ii) emit a phonon in energy level 2 to cool down to energy level 1 and then undergo CM, or (iii) emit a phonon in energy level 2 to cool down to energy level 1 and subsequently emit a phonon in energy level 1 to cool down below it. In all three scenarios, the electron ends up below level 1 and is no longer able to decay via CM. From this consideration we can calculate the relaxation time from each energy level to below level 1 for comparison to Figure 1a. The first relaxation times are given by

$$\tau_1 = p_{PE,1}\frac{1}{k_{tot,1}} + p_{CM,1}\frac{1}{k_{tot,1}} = \frac{1}{k_{tot,1}}$$
$$\tau_2 = p_{PE,2}p_{PE,1}\left(\frac{1}{k_{tot,2}} + \frac{1}{k_{tot,1}}\right) + p_{PE,2}p_{CM,1}\left(\frac{1}{k_{tot,2}} + \frac{1}{k_{tot,1}}\right) + p_{CM,2}\frac{1}{k_{tot,2}}$$
$$\tau_3 = p_{PE,3}p_{PE,2}p_{PE,1}\left(\frac{1}{k_{tot,3}} + \frac{1}{k_{tot,2}} + \frac{1}{k_{tot,1}}\right) + p_{PE,3}p_{PE,2}p_{CM,1}\left(\frac{1}{k_{tot,3}} + \frac{1}{k_{tot,2}} + \frac{1}{k_{tot,1}}\right) + p_{PE,3}p_{CM,2}\left(\frac{1}{k_{tot,3}} + \frac{1}{k_{tot,2}}\right) + p_{CM,3}\frac{1}{k_{tot,3}} \tag{2}$$

The corresponding QYs for comparison to Figure 1b can be calculated in a similar manner. Note that the QY is defined as the total number of charge carriers per absorbed photon. The QY is therefore always at least unity and becomes higher when CM occurs. The first QYs are given by

$$QY_1 = 1 + p_{CM,1} = 2 - p_{PE,1}$$
$$QY_2 = 1 + p_{CM,2} + p_{PE,2}p_{CM,1} = 2 - p_{PE,2}p_{PE,1}$$
$$QY_3 = 1 + p_{CM,3} + p_{PE,3}p_{CM,2} + p_{PE,3}p_{PE,2}p_{CM,1} = 2 - p_{PE,3}p_{PE,2}p_{PE,1} \tag{3}$$

The last right-hand side expressions in eq 3 indicate that CM occurs for all decay pathways, except for the case in which the electron cools down through all energy levels via phonon emission. For any initial energy level N (with energy such that only one CM event is possible), we can extend eqs 2 and 3 to a general result given by

$$\tau_N = \prod_{i=1}^{N}(p_{PE,i})\sum_{i=1}^{N}\left(\frac{1}{k_{tot,i}}\right) + \sum_{j=1}^{N-1}\left\{p_{CM,j}\prod_{k=j+1}^{N}(p_{PE,k})\left[\sum_{k=j}^{N}\left(\frac{1}{k_{tot,k}}\right)\right]\right\} + p_{CM,N}\frac{1}{k_{tot,N}} \tag{4}$$

$$QY_N = 2 - \prod_{i=1}^{N}(p_{PE,i}) \tag{5}$$

We note that eqs 4 and 5 can be modified to include multiple CM events, but they become much more complicated and are not easily fit to the experimental data anymore. We therefore choose to limit ourselves to the situation of a single CM event.

Relating Experiment and Fits. To fit eqs 4 and 5 to the experimental data in Figure 1a,b, we first need to relate the photoexcitation energy, $h\nu$, to the hot electron energy ΔE (see Figure 2a) above the theoretical energy threshold of CM. A straightforward assumption would be to divide the photon energy in excess of the band gap equally between the electron and hole. This however cannot explain a CM threshold below three times the band gap energy, such as observed in Figure 1b. We therefore choose to give all the photon excess energy over the band gap to the electron as an upper limit. Our previous work indicates the existence of transitions in which the photon excess energy is divided as such.[28,31] With this assumption ΔE can be related to the photoexcitation energy using

$$\Delta E = h\nu - 2E_{bg} = h\nu - 1.9\ \text{eV} \tag{6}$$

Rescaling the photoexcitation energy according to eq 6, the number of the energy level N can be determined for each photon energy using

$$N = \frac{\Delta E}{\delta E}\ (\text{rounded up since the lowest level corresponds to } N = 1) \tag{7}$$

Finally, we prescribe an energy dependence for the phonon emission and CM rate constants of the form

$$k_{PE} = \alpha_{PE}\Delta E^{\beta_{PE}}$$
$$k_{CM} = \alpha_{CM}\Delta E^{\beta_{CM}} \tag{8}$$

where the unit of α is $[\text{eV}^{-\beta}\ \text{ps}^{-1}]$ since we take ΔE in [eV] and β is dimensionless. This power law dependence is a heuristic function, that can however describe the general energy dependence suggested by theory quite well.[24] We have carried out the analysis using polynomial functions up to the third order as well but were able to describe the results most accurately using the power law dependence of eq 8.

To fit eqs 4 and 5 to the data of Figure 1a,b, we rescale the photoexcitation energy $h\nu$ to ΔE according to eq 6. This approach yields both the relaxation time τ and the QY as a function of ΔE (the electron excess energy minus one band gap, $\Delta E = E_N - E_1$ from Figure 2a). The relaxation time relevant to CM is however relaxation from the initial electron energy $\Delta E = h\nu - 2E_{bg}$ down to $\Delta E = 0$. The experimental relaxation time in Figure 1a equals cooling to the band edge ($\Delta E = -E_{bg}$). Hence, we subtract a constant from the experimental relaxation time, such that it is zero for $\Delta E = 0$. Any relaxation below this energy is not relevant for CM. Finally, we perform a global fit of eqs 4 and 5 to the experimental data of the relaxation time and the QY as a function of ΔE. We set the highest energy level N for each data point using eq 7 with a distance of δE = 17 meV between energy levels, equal to the LO phonon energy in PbSe.[32] The fit parameters we find from this procedure are the fit parameters α and β from eq 8. We note that fitting to only the relaxation time or the QY, there is freedom in the fits of k_{CM} and k_{PE} yielding large uncertainties in α and β. The global fit we perform here with coupled fit parameters does result in an accurate outcome. We

DOI: 10.1021/acsaem.8b01779
ACS Appl. Energy Mater. 2019, 2, 721−728

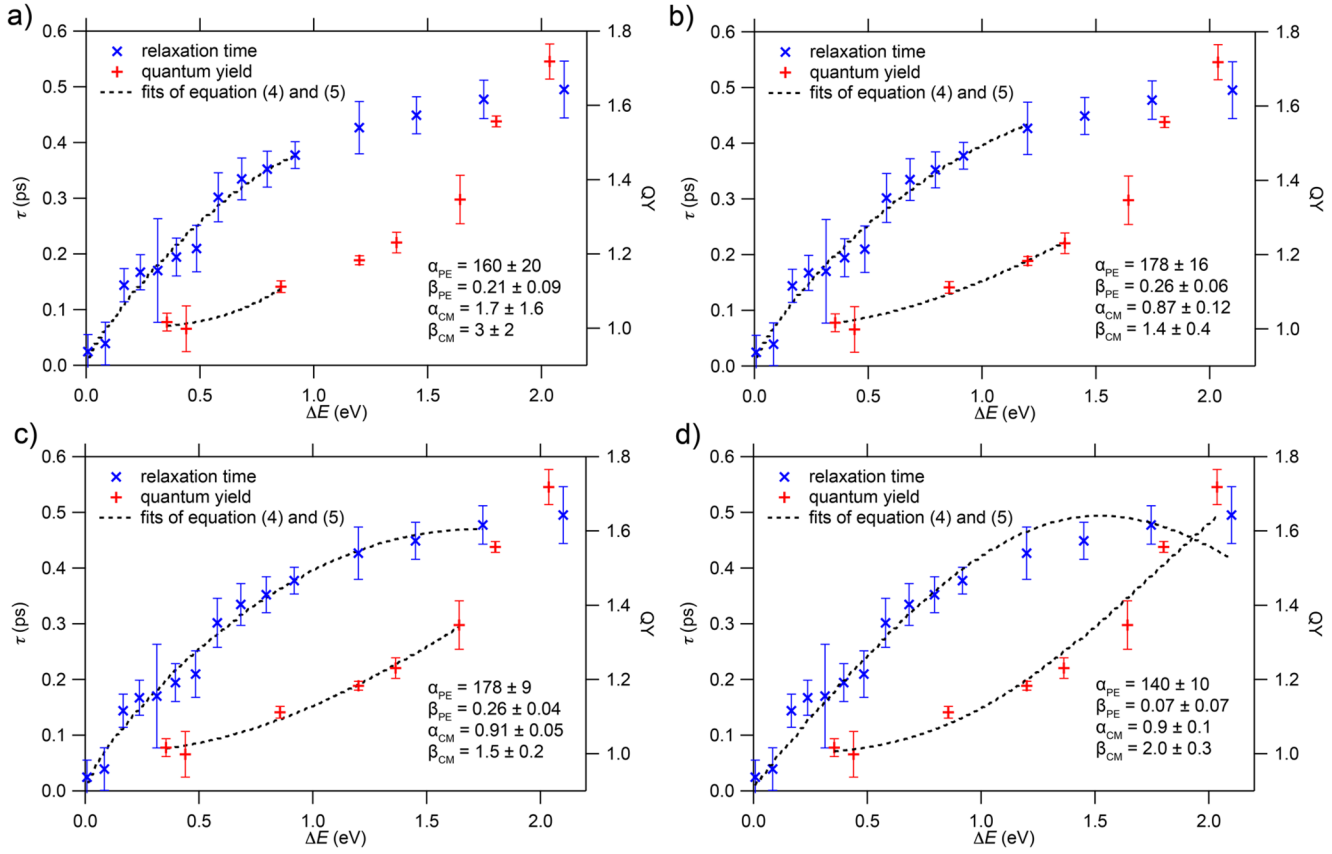

Figure 3. Fits of eqs 4 and 5 to the experimental data up to (a) ΔE < 0.95 eV, (b) ΔE < 1.4 eV, (c) ΔE < 1.7 eV, and (d) ΔE < 2.1 eV. Fit parameters from eq 8 are presented in the figures. The unit of α is $[\mathrm{eV}^{-\beta}\ \mathrm{ps}^{-1}]$, and β is dimensionless.

have included the code used to fit eqs 4 and 5 to the experimental data of the relaxation time and QY in the Supporting Information.

RESULTS AND DISCUSSION

Fits to the experimental data points for which ΔE < 0.95 eV are shown in Figure 3a, with the fitted parameters indicated in the figure. We choose this limit for ΔE because of the validity of our model for only a single CM event, as discussed above. We observe that the fit reproduces the experimental data, but with high uncertainties in the fit parameters up to 100%. The low maximum value of the QY = 1.11 suggests only a small contribution from multiple CM events. We can therefore extend the range of our analysis to experimental data points at ΔE > 0.95 eV. If we do so, we obtain values of the fit parameters in Figure 3b (ΔE < 1.4 eV) and Figure 3c (ΔE < 1.7 eV) in line with those previously obtained, but decreasing the uncertainty to a maximum of only 15% for the latter case. The maximum value of the QY = 1.35 in Figure 3c is evidently still small enough to neglect multiple CM events.

However, the fit becomes worse when we further extend its range to include the full experimental data (ΔE < 2.1 eV), see Figure 3d. Surprisingly, the fitted relaxation time even decreases with energy. This is due to neglecting multiple CM events. When CM occurs, the electron in our model is taken out of the analysis (moved to an energy level i < 1 in Figure 2a). For high enough energy, however, an electron can undergo CM to an energy level $i \geq 1$ from which CM can occur again. Therefore, this electron continues to cool down after the first CM event, increasing the total relaxation time. In our model, however, this electron is considered to be completely relaxed after the first CM event, resulting in a relaxation time that is shorter in the fit than in the experiment. Additionally, the CM rate constant increases with increasing energy according to eq 8. As the CM rate constant increases, on average fewer cooling events take place before the first CM event occurs. If the electron is taken out of the analysis after this first CM event as discussed above, the relaxation time can decrease with increasing energy such as observed in the fit of Figure 3d. Neglecting the relaxation time after the first CM event is too severe an approximation to describe the data for the highest ΔE. With a measured QY = 1.72, the scenario of multiple CM events is likely. We therefore trust our analysis only up to ΔE < 1.7 eV.

The distance, δE, between energy levels in the electronic structure of Figure 2a has an influence on the fit through eq 7. If the distance becomes too large, eqs 4 and 5 will yield a stepwise increase of, respectively, the relaxation time and the QY as a function of electron excess energy. In Figure 4a we show fits to our experimental data using eqs 4 and 5, for different values of δE. We reproduce the fits separately for visibility in the Supporting Information, Figure S1. We observe that for large δE, on the order of 100 meV, indeed the fits have a stepwise character and do not describe the data as well as the smoother fits for smaller δE. The fits for small δE all yield the same fit parameters α_{CM}, β_{CM}, and β_{PE}. Only α_{PE} increases from 178 for δE = 17 meV to 300 for δE = 10 meV to 600 for δE = 5 meV. This is to be expected, since the phonon emission rate is inversely dependent on the phonon energy δE if the average energy loss rate (i.e., the total relaxation time) remains constant (see eq 11 below). Since we argued before that δE

DOI: 10.1021/acsaem.8b01779
ACS Appl. Energy Mater. 2019, 2, 721−728

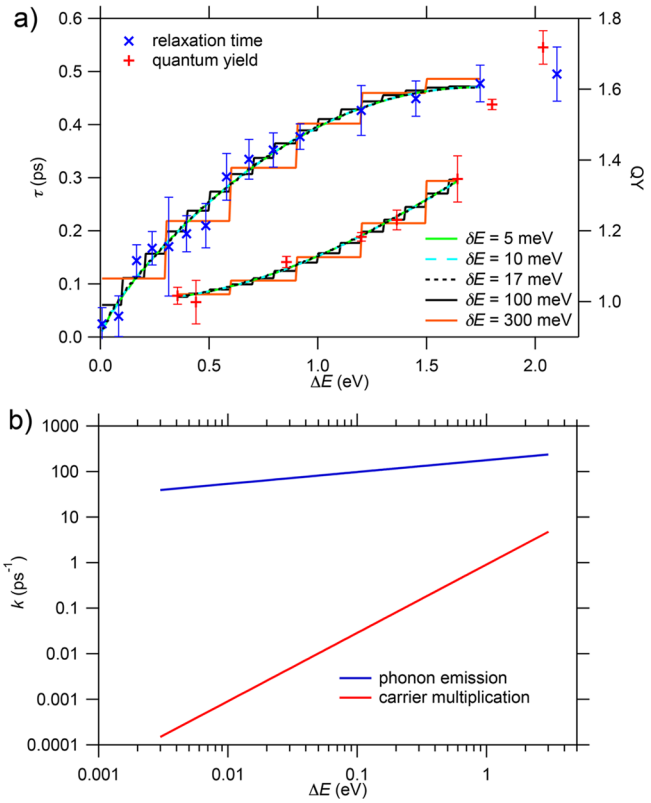

Figure 4. (a) Fits to the experimental data using eqs 4 and 5 with different values of δE. (b) Phonon emission rate constant for 17 meV LO phonons and experimental CM rate constant in 3.9 nm PbSe QDs.

represents the phonon energy, these results indicate that cooling in our model can be governed by the most energetic LO phonons with an energy of 17 meV as well as any other less energetic phonons. We consider LO phonons the most probable, since the most energy can be dissipated per step. Most importantly, the CM rate constant is invariant with the phonon energy δE, if it is small enough.

We finally find a phonon emission rate constant for 17 meV LO phonons and an experimental CM rate constant of

$$k_{PE} = (178 \pm 9)\Delta E^{(0.26\pm0.04)}\ \mathrm{ps}^{-1}$$
$$k_{CM} = (0.91 \pm 0.05)\Delta E^{(1.5\pm0.2)}\ \mathrm{ps}^{-1} \quad (9)$$

in 3.9 nm PbSe QDs, with ΔE in eV. We show these rates as a function of ΔE in Figure 4b. The energy dependence of the CM rate constant should be related to both the Coulomb matrix element for CM at the energy of the hot electron and the density of final biexciton states through Fermi's Golden Rule. Theoretical calculations using various methods either find similar[27] or higher[24,25] CM rate constants than the experimental CM rate constant we find. We are uncertain what exactly causes the discrepancy. We note however that the joint DOS for electrons and holes upon photon absorption in a single, parabolic band semiconductor scales with $(h\nu - E_{bg})^{0.5}$ and can be higher when more bands are involved.[33]

The above method is applicable to any material for which the required experimental data is available, taking into account the following considerations. One should consider carefully how to divide the excess photon energy between the electron and hole for materials in which an asymmetric distribution is less likely than in PbSe QDs. Moreover, depending on theoretical insights and the quality of the fits, the prescribed energy dependence of the rate constants as given in eq 8 could be chosen differently to suit the material under investigation. Finally, eqs 4 and 5 can be modified to include multiple CM events, although this greatly increases their complexity.

Estimate of the CM Rate Constant from the QY. The above analysis yields phonon emission and experimental CM rate constants as a function of electron excess energy from experimental data of the relaxation time and QY in QDs. The major limitation of eq 4 is that it requires detailed experimental data of the relaxation time up to high photoexcitation energy. In literature, such data is very rare. The data of the QY needed for eq 5 is much more common for many different materials. We therefore discuss here a simplified method to estimate the CM rate constant just above the energetic threshold of CM using only experimental data of the QY.

We first need to estimate an energy loss rate. With the experimental data of the relaxation time from Figure 1a, we can calculate an average energy loss rate γ in an energy interval ΔE using

$$\gamma = \frac{dE}{dt} = \left[\frac{d\tau}{d(h\nu)}\right]^{-1} \approx \frac{\Delta E}{\Delta \tau} \quad (10)$$

where τ is the relaxation time and $h\nu$ the photon energy. We wish to use this average energy loss rate for estimating a phonon emission rate constant in the electronic structure of Figure 2a. If relaxation is only governed by phonon emission, then

$$k_{PE} = \frac{\gamma}{\delta E} = N\frac{\gamma}{\Delta E} \quad (11)$$

The phonon emission rate in eq 11 is inversely dependent on the phonon energy δE, as mentioned before when we discussed Figure 4a. Equation 11 neglects any energy lost through CM and is therefore only valid below the onset of CM. We however approximate k_{PE} just above the energetic threshold of CM with k_{PE} calculated using eq 11.

The benefit of eqs 10 and 11 is that an energy loss rate and consequently a phonon emission rate constant can be estimated from experimental data or theoretical calculations. This can then be used to estimate a CM rate constant just above the onset of CM. Of course this simplified method is not as accurate as applying the entire method discussed above and does not yield a full energy dependence of the CM rate constant, but it aids in further analyzing existing experimental data.

To find a CM rate constant, we next consider how an electron relaxes through the electronic structure of Figure 2a. The probabilities given in eq 1 that an electron either undergoes CM or cools from a given energy level by emitting a phonon are now constant, because of the average energy loss rate used from eq 10. Consequently, the probability that a hot electron created in energy level N does not undergo CM and therefore relaxes to below level 1 by emitting N phonons is equal to $(p_{PE})^N$. In all other scenarios, the electron undergoes CM. The total probability of an electron undergoing CM in any of the energy levels is therefore $1 - (p_{PE})^N$. As such, the QY is given by (recall that the QY is one plus the yield from CM)

DOI: 10.1021/acsaem.8b01779
ACS Appl. Energy Mater. 2019, 2, 721−728

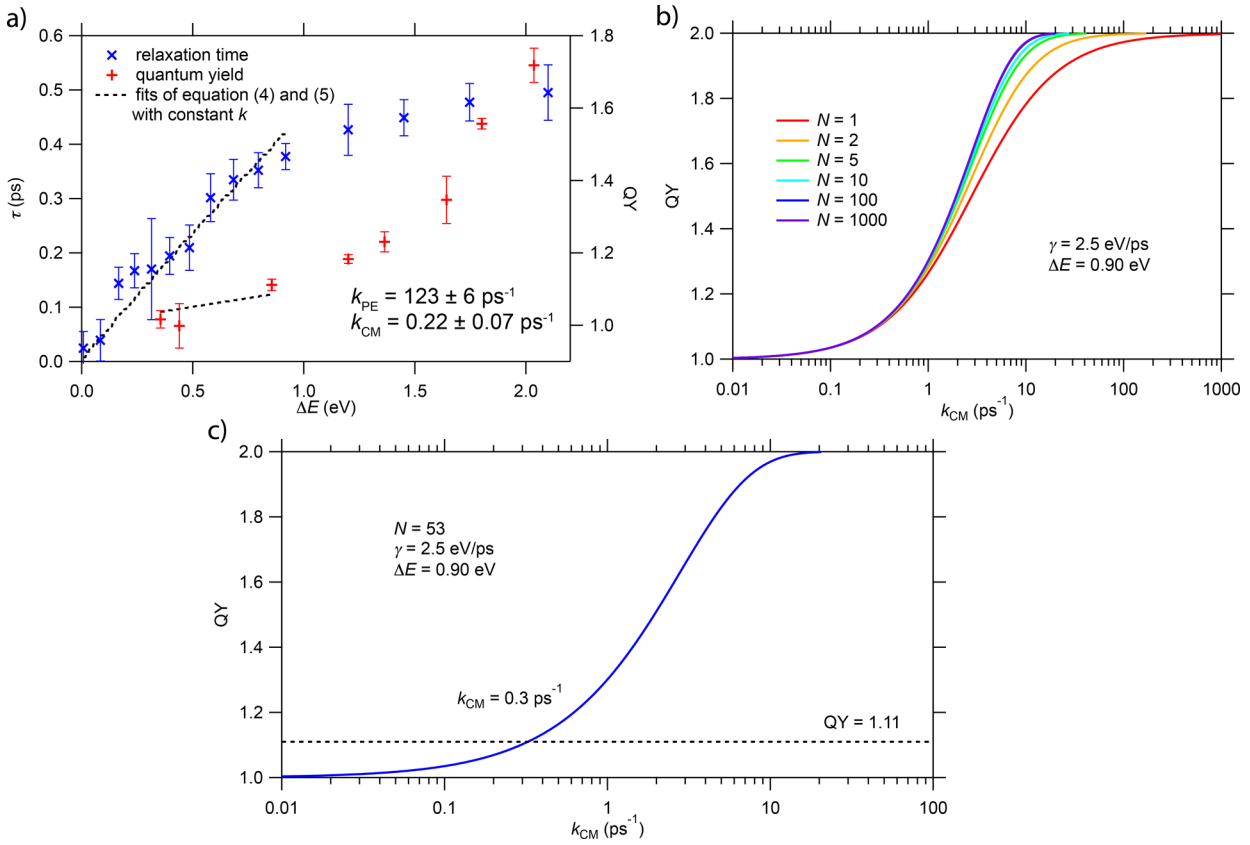

Figure 5. (a) Fits to the experimental data using eqs 4 and 5 for constant phonon emission and CM rate constants. (b) QY as a function of k_{CM}, calculated using eq 12, for γ = 2.5 eV/ps, ΔE = 0.90 eV, and various N. The QY converges for N > 10. (c) QY as a function of k_{CM}, calculated using eq 12, for γ = 2.5 eV/ps, ΔE = 0.90 eV, and N = 53. The QY = 1.11 is indicated by the black dashed line and intersects the solution from eq 12 at k_{CM} = 0.3 ps^{-1}.

$$\mathrm{QY} = 2 - \left(\frac{k_{PE}}{k_{PE} + k_{CM}}\right)^{N} \tag{12}$$

Equation 12 is used to estimate the CM rate constant from experimental data of the QY. It requires an estimate of the phonon emission rate constant from eq 11 as discussed above. Note that according to eq 12, the CM rate constant becomes comparable to the phonon emission rate constant if the QY significantly exceeds unity. Since we neglected energy lost through CM in eq 11, we again observe that eq 12 is only valid just above the onset of CM.

We compare the simplified model discussed above to the full model of eqs 4 and 5 for our experimental data of the relaxation time and QY in 3.9 nm PbSe QDs. We show in Figure 5a fits of the full model to the experimental data prescribing constant phonon emission and CM rate constants, up to the first data point of the QY exceeding unity. The fitted rate constants are included in the figure. We observe from Figure 5a that the fits of the relaxation time and QY increase linearly with ΔE, as expected for constant rate constants.

To use eq 12, we need to find reasonable values for γ and N. From Figure 5a, we observe that for the first QY data point exceeding unity, ΔE = 0.90 eV. Using eq 10 we find from the relaxation time that γ = 2.5 eV/ps for $0 \leq \Delta E \leq 0.90$ eV. With these parameters, we show the QY calculated using eq 12 as a function of k_{CM} in Figure 5b for different N.

From Figure 5b, we observe that the QY calculated using eq 12 depends on N but converges for N > 10. If we consider the distance between energy levels, δE, equal to the LO phonon energy in PbSe of 17 meV as before, we find from eq 11 that N = 53 and k_{PE} = 147 ps^{-1}. With these values of the parameters, we again show the QY calculated using eq 12 as a function of k_{CM} in Figure 5c. We also indicate QY = 1.11 with a black dashed line, equal to the first experimental QY data point exceeding unity. From Figure 5c we observe that k_{CM} = 0.3 ps^{-1} for the QY = 1.11.

We observe from Figure 5a,c that the CM rate constants determined from our full fit procedure with constant rate constants and from using eq 12 are equal within the error margin. We therefore find k_{CM} = 0.3 ps^{-1} as an estimate just above the energetic threshold of CM. Note that k_{CM} is indeed much smaller than k_{PE}, in agreement with the assumption to obtain eq 11.

For ΔE = 0.90 eV, we find from eq 9 that k_{CM} = 0.8 ps^{-1} and k_{PE} = 174 ps^{-1} using the full model of eqs 4 and 5 and both the experimental relaxation time and QY. The simplified method using eq 12 therefore significantly underestimates the CM rate constant. It is however useful to estimate an order-of-magnitude for the CM rate constant when only experimental data of the QY is available.

CONCLUSIONS

We have presented a method to determine the rate constant of CM for initially hot charge carriers from experimental data of the relaxation time and QY. We have illustrated this method for electrons in 3.9 nm PbSe QDs, for which we find a CM rate of $k_{CM} = (0.91 \pm 0.05)\Delta E^{(1.5\pm0.2)}$ ps^{-1} with ΔE in eV. We have

DOI: 10.1021/acsaem.8b01779
ACS Appl. Energy Mater. 2019, 2, 721−728

also derived a simplified method to estimate the CM rate constant just above the onset of CM when only experimental data of the QY is available. The method to determine the CM rate constant is generally applicable to analyze the observed CM efficiency in quantum confined and bulk materials. Extraction of a distinct CM rate constant can be useful for screening and direct development of materials with enhanced CM efficiency.

■ ASSOCIATED CONTENT

Supporting Information

The Supporting Information is available free of charge on the ACS Publications website at DOI: 10.1021/acsaem.8b01779.

Code used for fitting eqs 4 and 5 to experimental data of the relaxation time and QY and reproduction of Figure 4a for each fit separately (PDF)

■ AUTHOR INFORMATION

Corresponding Authors

*E-mail: A.J.Houtepen@tudelft.nl.

*E-mail: L.D.A.Siebbeles@tudelft.nl.

ORCID

Gianluca Grimaldi: 0000-0002-2626-9118

Arjan J. Houtepen: 0000-0001-8328-443X

Laurens D. A. Siebbeles: 0000-0002-4812-7495

Author Contributions

§F.C.M.S. and G.G. share first authorship. F.C.M.S. and G.G. performed the measurements, developed the model, and carried out the analysis. A.J.H. and L.D.A.S. managed the project. The manuscript was written through contributions of all authors. All authors have given approval to the final version of the manuscript.

Notes

The authors declare no competing financial interest.

■ ACKNOWLEDGMENTS

F.C.M.S. and L.D.A.S. were supported by the Dutch Foundation for Fundamental Research on Matter (FOM) with the Project "Hot Electrons in Cool Nanocrystals". G.G., S.K., A.J.H., and L.D.A.S. were supported by STW (Project No. 13903, Stable and Non-Toxic Nanocrystal Solar Cells). A.J.H. was supported by ERC STG "Doping-on-Demand".

■ ABBREVIATIONS

QD, quantum dot
CM, carrier multiplication
QY, quantum yield
DOS, density-of-states
VB, valence band
CB, conduction band

■ REFERENCES

(1) Smith, C.; Binks, D. Multiple Exciton Generation in Colloidal Nanocrystals. *Nanomaterials* **2014**, *4* (1), 19−45.

(2) Kershaw, S.; Rogach, A. Carrier Multiplication Mechanisms and Competing Processes in Colloidal Semiconductor Nanostructures. *Materials* **2017**, *10* (9), 1095.

(3) Padilha, L. A.; Stewart, J. T.; Sandberg, R. L.; Bae, W. K.; Koh, W.-K.; Pietryga, J. M.; Klimov, V. I. Carrier Multiplication in Semiconductor Nanocrystals: Influence of Size, Shape, and Composition. *Acc. Chem. Res.* **2013**, *46* (6), 1261−1269.

(4) Trinh, M. T.; Houtepen, A. J.; Schins, J. M.; Hanrath, T.; Piris, J.; Knulst, W.; Goossens, A. P. L. M.; Siebbeles, L. D. A. In spite of recent doubts carrier multiplication does occur in PbSe nanocrystals. *Nano Lett.* **2008**, *8* (6), 1713−1718.

(5) Aerts, M.; Suchand Sandeep, C. S.; Gao, Y.; Savenije, T. J.; Schins, J. M.; Houtepen, A. J.; Kinge, S.; Siebbeles, L. D. A. Free Charges Produced by Carrier Multiplication in Strongly Coupled PbSe Quantum Dot Films. *Nano Lett.* **2011**, *11* (10), 4485−4489.

(6) Suchand Sandeep, C. S.; ten Cate, S.; Schins, J. M.; Savenije, T. J.; Liu, Y.; Law, M.; Kinge, S.; Houtepen, A. J.; Siebbeles, L. D. High charge-carrier mobility enables exploitation of carrier multiplication in quantum-dot films. *Nat. Commun.* **2013**, *4*, 2360.

(7) Padilha, L. A.; Stewart, J. T.; Sandberg, R. L.; Bae, W. K.; Koh, W.-K.; Pietryga, J. M.; Klimov, V. I. Aspect Ratio Dependence of Auger Recombination and Carrier Multiplication in PbSe Nanorods. *Nano Lett.* **2013**, *13* (3), 1092−1099.

(8) Aerts, M.; Bielewicz, T.; Klinke, C.; Grozema, F. C.; Houtepen, A. J.; Schins, J. M.; Siebbeles, L. D. A. Highly efficient carrier multiplication in PbS nanosheets. *Nat. Commun.* **2014**, *5*, 3789.

(9) Kulkarni, A.; Evers, W. H.; Tomic, S.; Beard, M. C.; Vanmaekelbergh, D.; Siebbeles, L. D. A. Efficient Steplike Carrier Multiplication in Percolative Networks of Epitaxially Connected PbSe Nanocrystals. *ACS Nano* **2018**, *12* (1), 378−384.

(10) Pijpers, J. J. H.; Ulbricht, R.; Tielrooij, K. J.; Osherov, A.; Golan, Y.; Delerue, C.; Allan, G.; Bonn, M. Assessment of carrier-multiplication efficiency in bulk PbSe and PbS. *Nat. Phys.* **2009**, *5* (11), 811−814.

(11) Gabor, N. M.; Zhong, Z.; Bosnick, K.; Park, J.; McEuen, P. L. Extremely Efficient Multiple Electron-Hole Pair Generation in Carbon Nanotube Photodiodes. *Science* **2009**, *325* (5946), 1367−1371.

(12) Semonin, O. E.; Luther, J. M.; Choi, S.; Chen, H. Y.; Gao, J. B.; Nozik, A. J.; Beard, M. C. Peak External Photocurrent Quantum Efficiency Exceeding 100% via MEG in a Quantum Dot Solar Cell. *Science* **2011**, *334* (6062), 1530−1533.

(13) Davis, N.; Bohm, M. L.; Tabachnyk, M.; Wisnivesky-Rocca-Rivarola, F.; Jellicoe, T. C.; Ducati, C.; Ehrler, B.; Greenham, N. C. Multiple-exciton generation in lead selenide nanorod solar cells with external quantum efficiencies exceeding 120%. *Nat. Commun.* **2015**, *6*, 8259.

(14) Barati, F.; Grossnickle, M.; Su, S.; Lake, R. K.; Aji, V.; Gabor, N. M. Hot carrier-enhanced interlayer electron−hole pair multiplication in 2D semiconductor heterostructure photocells. *Nat. Nanotechnol.* **2017**, *12*, 1134.

(15) Yan, Y.; Crisp, R. W.; Gu, J.; Chernomordik, B. D.; Pach, G. F.; Marshall, A. R.; Turner, J. A.; Beard, M. C. Multiple exciton generation for photoelectrochemical hydrogen evolution reactions with quantum yields exceeding 100%. *Nat. Energy* **2017**, *2* (5), 17052.

(16) Kambhampati, P. Hot Exciton Relaxation Dynamics in Semiconductor Quantum Dots: Radiationless Transitions on the Nanoscale. *J. Phys. Chem. C* **2011**, *115* (45), 22089−22109.

(17) Stewart, J. T.; Padilha, L. A.; Qazilbash, M. M.; Pietryga, J. M.; Midgett, A. G.; Luther, J. M.; Beard, M. C.; Nozik, A. J.; Klimov, V. I. Comparison of Carrier Multiplication Yields in PbS and PbSe Nanocrystals: The Role of Competing Energy-Loss Processes. *Nano Lett.* **2012**, *12* (2), 622−628.

(18) Stewart, J. T.; Padilha, L. A.; Bae, W. K.; Koh, W. K.; Pietryga, J. M.; Klimov, V. I. Carrier Multiplication in Quantum Dots within the Framework of Two Competing Energy Relaxation Mechanisms. *J. Phys. Chem. Lett.* **2013**, *4* (12), 2061−8.

(19) Beard, M. C.; Midgett, A. G.; Hanna, M. C.; Luther, J. M.; Hughes, B. K.; Nozik, A. J. Comparing multiple exciton generation in quantum dots to impact ionization in bulk semiconductors: implications for enhancement of solar energy conversion. *Nano Lett.* **2010**, *10* (8), 3019−27.

(20) Park, J.; Joo, J.; Kwon, S. G.; Jang, Y.; Hyeon, T. Synthesis of Monodisperse Spherical Nanocrystals. *Angew. Chem., Int. Ed.* **2007**, *46* (25), 4630−4660.

(21) Cho, B.; Peters, W. K.; Hill, R. J.; Courtney, T. L.; Jonas, D. M. Bulklike hot carrier dynamics in lead sulfide quantum dots. *Nano Lett.* **2010**, *10* (7), 2498−505.
(22) Miaja-Avila, L.; Tritsch, J. R.; Wolcott, A.; Chan, W. L.; Nelson, C. A.; Zhu, X. Y. Direct mapping of hot-electron relaxation and multiplication dynamics in PbSe quantum dots. *Nano Lett.* **2012**, *12* (3), 1588−91.
(23) Spoor, F. C. M.; Tomic, S.; Houtepen, A. J.; Siebbeles, L. D. A. Broadband cooling spectra of hot electrons and holes in PbSe quantum dots. *ACS Nano* **2017**, *11* (6), 6286−6294.
(24) Allan, G.; Delerue, C. Role of impact ionization in multiple exciton generation in PbSe nanocrystals. *Phys. Rev. B: Condens. Matter Mater. Phys.* **2006**, *73* (20), 205423.
(25) Franceschetti, A.; An, J. M.; Zunger, A. Impact ionization can explain carrier multiplication in PbSe quantum dots. *Nano Lett.* **2006**, *6* (10), 2191−2195.
(26) Rabani, E.; Baer, R. Theory of multiexciton generation in semiconductor nanocrystals. *Chem. Phys. Lett.* **2010**, *496* (4), 227−235.
(27) Velizhanin, K. A.; Piryatinski, A. Numerical Study of Carrier Multiplication Pathways in Photoexcited Nanocrystal and Bulk Forms of PbSe. *Phys. Rev. Lett.* **2011**, *106* (20), 207401.
(28) Spoor, F. C. M.; Grimaldi, G.; Delerue, C.; Evers, W. H.; Crisp, R. W.; Geiregat, P.; Hens, Z.; Houtepen, A. J.; Siebbeles, L. D. A. Asymmetric Optical Transitions Determine the Onset of Carrier Multiplication in Lead Chalcogenide Quantum Confined and Bulk Crystals. *ACS Nano* **2018**, *12*, 4796.
(29) Allan, G.; Delerue, C. Confinement effects in PbSe quantum wells and nanocrystals. *Phys. Rev. B: Condens. Matter Mater. Phys.* **2004**, *70* (24), 245321.
(30) An, J. M.; Franceschetti, A.; Dudiy, S. V.; Zunger, A. The peculiar electronic structure of PbSe quantum dots. *Nano Lett.* **2006**, *6* (12), 2728−35.
(31) Spoor, F. C. M.; Kunneman, L. T.; Evers, W. H.; Renaud, N.; Grozema, F. C.; Houtepen, A. J.; Siebbeles, L. D. A. Hole Cooling Is Much Faster than Electron Cooling in PbSe Quantum Dots. *ACS Nano* **2016**, *10* (1), 695−703.
(32) Geiregat, P.; Delerue, C.; Justo, Y.; Aerts, M.; Spoor, F.; Van Thourhout, D.; Siebbeles, L. D. A.; Allan, G.; Houtepen, A. J.; Hens, Z. A Phonon Scattering Bottleneck for Carrier Cooling in Lead Chalcogenide Nanocrystals. *ACS Nano* **2015**, *9* (1), 778−788.
(33) Fox, M. *Optical Properties of Solids*; Oxford University Press: Oxford, U.K., 2001.

DOI: 10.1021/acsaem.8b01779
ACS Appl. Energy Mater. 2019, 2, 721−728